RSC Advances

PAPER

View Article Online
View Journal | View Issue

Cite this: *RSC Adv.*, 2020, **10**, 5371

LC-MS analysis of *Myrica rubra* extract and its hypotensive effects *via* the inhibition of GLUT 1 and activation of the NO/Akt/eNOS signaling pathway†

Jing Li, ‡ Huiling Wang,‡ Jian Li, Yonggang Liu and Hong Ding *

Received 30th July 2019
Accepted 5th January 2020

DOI: 10.1039/c9ra05895h

rsc.li/rsc-advances

In the area of medicine food homology, *Myrica rubra* ((Lour.) Siebold & Zucc.) has been used in medicine as an astringent and anti-diarrheal. However, there are few in-depth studies evaluating the antihypertensive chemical components and antihypertensive mechanisms of *Myrica rubra*. Thus, the aim in this study was to assess the protective effects of an ethanol extract of bayberry (BE) on spontaneous hypertension in rats. In this study, liquid chromatography-mass spectroscopy (LC-MS) coupled with biochemical assays and western blot have been employed to study the protective effects of BE against hypertension. A total of 28 compounds were identified in BE. According to this study, treatment with BE (2 g kg^{-1}) resulted in the potent and persistent reduction of high blood pressure, even after drug withdrawal. The results indicate that the mechanisms of action might involve protection against damage to the vascular structure. Bayberry extract could enhance the endothelium-independent vascular function, inhibiting the abnormal proliferation of smooth muscle by inhibition of glucose transporter-1 (GLUT 1) and regulation of nitric oxide (NO)/serine/threonine kinases (Akt)/endothelial nitric oxide synthase (eNOS). The results of molecular docking and *in vitro* research indicated six compounds in BE that might be responsible for the antihypertensive effect attributed to GLUT 1, eNOS and Akt, and further *in vivo* studies are needed to verify this.

1. Introduction

Hypertension is a common condition that causes cardiovascular disease and related complications, such as stroke, heart attack and heart failure. It is often accompanied by metabolic disorders, especially dyslipidemia.[1] Every year, approximately 17 million people worldwide die from cardiovascular disease, accounting for nearly one-third of all deaths. Of these, 9.4 million deaths are caused by complications from hypertension. In 2008, global statistics showed that 40% of adults aged 25 and over were diagnosed with high blood pressure.[2,3] According to recent health reports, hypertension is considered to be a worldwide health concern that will affect 1.56 billion people by 2025.[4]

The pathogenesis of hypertension is complex, and most forms of hypertension lead to increased vasomotor tension, resulting in an increase in total peripheral resistance.[5] Nitric oxide (NO) synthesized from L-arginine by nitric oxide synthase (NOS) plays a key role in regulating blood flow, blood pressure and oxygen delivery.[6] Endothelial NOS (eNOS) is a key rate-limiting enzyme in NO formation. The expression and biological activity of eNOS directly affects the formation of NO.[7] NOS contains neuronal NOS (nNOS), inducible NOS (iNOS) and eNOS.[8] Angiotensin II (Ang II) is a peptide hormone of the renin–angiotensin–aldosterone system and causes pleiotropic effects on the vasculature. As an effective vasoconstrictor, it acts by the Ang II receptor 1, which is mainly expressed on resistance vessels, and thus Ang II increases peripheral resistance to enhance blood pressure. Thus, increase in Ang II signaling is considered to be a strong stimulus for arterial aging, and Ang II affects the structural, molecular, functional, and biomechanical properties of the arterial wall.[9–11]

Blood pressure (BP) is controlled by the renin–angiotensin system, in which the renin-derived, renin-catalyzed rate of angiotensinogen conversion to angiotensin I (AT-I) is limited by an inactive decapeptide. Angiotensin-converting enzyme (ACE) plays a crucial role in the regulation of blood pressure, and catalyzes the cleavage of the carboxy-terminal His–Leu dipeptide of AT-1 into angiotensin II, which is an effective octapeptide vasopressor.[12] Recently, studies have shown that inflammation plays a crucial role in the development of essential hypertension.[13,14] Tumor necrosis factor-α (TNF-α) stimulates the

Key Laboratory of Combinatorial Biosynthesis and Drug Discovery, Ministry of Education, School of Pharmaceutical Sciences, Wuhan University, Wuhan, 430071, China. E-mail: dinghong1106@whu.edu.cn; Tel: +8613007162084

† Electronic supplementary information (ESI) available: Chemical structures of main components identified in the extract of *Myrica rubra*. Proposed fragmentation patterns pathway of quercetin-3-*O*-2′,6′-dirhamnosylglucoside. The cellular viability of H_2O_2-induced HUVECs injury with compounds **1**, **3**, **4**, **7**, **8**, **9**, **11**, **12**, **19**, **21**, **23**, **27** at different concentrations. See DOI: 10.1039/c9ra05895h

‡ These authors contributed equally.

production of cytokines, enhances the expression of adhesion molecules and increases the activation of neutrophils. In 2008, Navarro-González *et al.*[15] found that serum TNF-α levels were higher in hypertensive patients than in healthy controls.

Among the available antihypertensive drugs, diuretics, ACE inhibitors, calcium-channel blockers and also alpha- and beta-blocker drugs are the first choice of treatment for mild to moderate hypertension. Like most synthetic drugs they have long-lasting adverse effects, including cough, high blood sugar, weakness/fatigue, rash, kidney damage and so on.[16] Considering increasing awareness of high blood pressure, healthier lifestyles are being introduced to the public, such as eating a balanced diet, reducing salt and alcohol intake, and reducing tobacco use. It is easy to achieve the desired state of health by controlling the type of food people consume. Under these circumstances, the functional food market, which was once a niche market, is booming. The demand for healthier food has prompted food scientists to try to develop a food system that can treat hypertension, beyond the basic nutrients of carbohydrates, protein and fat.

Historically, traditional herbal medicines have been the treatment strategy for Chinese medical systems to treat a variety of diseases. However, *Myrica rubra* is rarely used to treat high blood pressure, and few studies have reported its mechanism of action for blood pressure. The Chinese bayberry,[17] which is used in medicine and food, is a plant of the genus *Myrica* distributed in East Asia. It has been planted in southern China for more than 2000 years. The leaves, bark and fruit of the tree have astringent effects, antihypertensive effects, detoxification effects and anti-diarrheal effects in Chinese medicine.[18,19] In addition, bayberry extracts show other biological activities such as liver protection,[20] antioxidant activity,[21] and antiviral effects.[22] The main groups of secondary metabolites are flavonoids, tannins,[23] triterpenoids[24] and diarylheptanoid acid.[25]

The aim of this study was to assess the protective effect of BE on spontaneous hypertension in rats (SHR) and its potential mechanism of action based on a novel strategy that incorporates LC-MS, western blotting and molecular docking. As far as we know, this is the first in-depth study to evaluate the antihypertensive chemical components and antihypertensive mechanisms of BE.

2. Materials and methods

2.1 Chemicals and reagents

Ethanol (EtOH) (95%) was purchased from Tianjin University Chemical experimental factory (Tianjin, China). Chromatographic grade acetonitrile and methanol were obtained from ThermoFisher (USA). Sodium 3-trimethylsilyl [2,2,3,3-d_4] propionate (TSP) was acquired from Cambridge Isotope Laboratories Inc. (Andover, MA, USA). Deuterated water (D_2O) was purchased from Norell (Landisville, NJ, USA). N^{ω}-Nitro-L-arginine methyl ester (L-NAME, >99%), analytical grade $Na_2HPO_4 \cdot 2H_2O$ and $NaH_2PO_4 \cdot 12H_2O$ were obtained, respectively, from Guangfu Fine Chemical Research Institute (Tianjin, China) and Zhiyuan Chemical Reagent Co., Ltd (Tianjin, China). Phosphate buffer was prepared with $Na_2HPO_4 \cdot 2H_2O$ and $NaH_2PO_4 \cdot 12H_2O$ (0.1 M, pH 7.4), containing 10% D_2O and 0.1 mM L^{-1} of TSP. All other reagents and chemicals were of analytical grade.

Anti-eNOS, anti-Akt, anti-eNOS, and anti-eAkt were the products from Boster (Wuhan, China), whereas fluorescein isothiocyanate (FITC)-conjugated goat anti-rabbit IgG was purchased from Beyotime Biotechnology (Jiangsu, China). Antibodies of eNOS-Ser^{1177} and Akt-Ser^{473} were purchased from Cell Signaling Technology (Boston, USA). The anti-rabbit IgG conjugated to horseradish peroxide was purchased from Santa Cruz Biotechnology (Texas, USA). Enzyme-linked immunosorbent assay (ELISA) kits were manufactured by Nanjing Jiancheng Biotechnology (Nanjing, China).

The bayberry was bought from a local drugstore and identified as *Myrica rubra* (Sieb. & Zucc.), which was deposited in Wuhan University. The survey was initiated by Prof. Hong Ding. Human umbilical vein endothelial cells (HUVECs) were purchased from the China Centre for Type Culture Collection.

2.2 Extract preparation

The bayberry was extracted three times with 95% EtOH (85 °C, 2 h each) reflux, and the combined extract was concentrated under reduced pressure for further chemical analysis and animal experiments.

2.3 LC-MS analysis of BE

The chemical composition of the BE was identified by LC-MS. BE was analyzed on the UHPLC Q Exactive Orbitrap MS equipment (ThermoFisher, USA). A ThermoFisher U3000 system was installed with a Waters BEH C18 column (2.1 mm × 100 mm, 1.7 μm) with an electrospray ionization ion source. The Z-spray ionization source was maintained at 300 °C and the spray voltage was kept at 3.5 kV in positive ionization mode. Additional operating parameters were capillary temperature: 320 °C, lens voltage: 55 kPa, mass resolution: 70 000, and mass scan range: 100–1500 m/z in full-scan mode.

Separation of biological samples was carried out at a flow rate of 0.2 mL min^{-1} and a column temperature of 30 °C, with an injection volume of 5 μL and a detection wavelength of 210 nm. The mobile phase was composed of (A) 0.1% formic acid aqueous solution and (B) acetonitrile at a flow rate of 0.2 mL min^{-1}, and the gradient elution was optimized as follows: 0–5 min, 5–15% B; 5–10 min, 15–20% B; 10–15 min, 25–35% B; 15–20 min, 35–40% B; 40–60% B; 24–24.5 min, 60–5% B; 24.5–27 min, 5% B.

2.4 Animal experiments

Eight-week-old male SHR and SD rats (180–220 g) were purchased from Beijing Vital River Laboratories Co., Ltd. (SCXK (Jing) 2016-0006, Beijing, China). After 1 week of domestication, eight male SD rats were treated as the control group, and the normotensive group was given a basic diet. Forty-eight male SHR rats were randomly divided into the following six groups (n = 8): SHR, rats were given distilled water; SHR-nifedipine (Ni), rats were administered with 10 mg kg^{-1} nifedipine; SHR-low dose (LD), rats were administered BE at a dosage of 1 g kg^{-1}; SHR-medium dose (MD), rats were administered with 2 g kg^{-1}

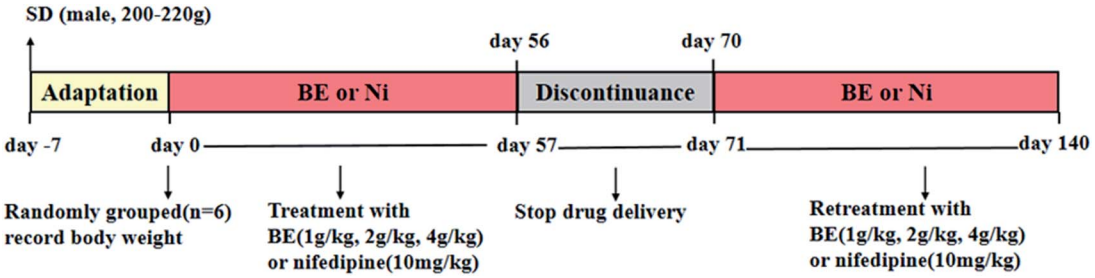

Fig. 1 SHR rat treatment with nifedipine (Ni) and bayberry extract (BE).

BE; SHR-high dose (HD), rats were administered with 4 g kg^{-1} BE. All groups were given a free diet. The procedures employed for the treatment with BE are shown in Fig. 1. The rats were kept in well-ventilated rooms, at temperatures of 25 ± 2 °C, in cycles of light and dark of 12 hours, and with relative humidity between 60 and 80%. All experiments were conducted according to the guidelines of the University of Houston and protocols were approved by Institutional Animal Care and Use Committee (IACUC), Wuhan University Center for Animal Experiment, Wuhan, China (AUP no. S201411012I).

2.5 Bodyweight

The bodyweight of every rat was recorded at 14:30 every two days throughout the whole experiment, so that we could supervise the body condition of each rat.

2.6 Blood pressure variability

A blood pressure analysis system (Tai Meng Scientific and Technologic Co., Ltd, Chengdu, China) was used to measure systolic blood pressure (SBP), diastolic blood pressure (DBP) and mean blood pressure (MBP) of awake rats every week, following establishment of the model. The final value was calculated from eight successive measurements.

2.7 Histology and morphological analyses of thoracic aorta and kidney

The thoracic aorta and kidney were fixed with 10% (v/v) neutral formalin for 48 hours. To enhance the fixation effect, the thoracic aorta and kidney were placed in rubber-covered ampoules and filled with 10% (v/v) neutral formalin to two-thirds of the maximum volume. The thoracic aorta were embedded in paraffin, sectioned at 4 μm, and stained with hematoxylin and eosin (H&E) and Verhoeff's Van Gieson stain (EVG) to observe the change. After administration, the effect on the kidney was observed by Masson's trichrome staining. Images were obtained and studied under light microscopy. Each part was magnified 100 times, and a random slide was taken from each set of eight animals.

2.8 Electron microscope scanning of thoracic aorta

A Philips XL30E scanning electron microscope (SEM) was used to detect the endothelial surface of various arteries, the images were scanned, and the degree of injury was observed.

2.9 Determination of biochemical index levels

After anesthesia, the femoral artery of rats was taken for blood supply, and serum was prepared by centrifugation at 13 000 rpm for 10 min. Serum was stored at −80 °C for further analysis. The levels of NO, Ang II, endothelin 1 (ET-1) and TNF-α were determined with the corresponding ELISA kits according to the manufacturer's instructions.

2.10 Immunohistological staining

To estimate the expression of GLUT 1 and eNOS proteins in the blood vessels, immunofluorescence and immunohistochemical staining were used, with reference to the literature.[26] Images were randomly captured by using an inverted fluorescent microscope (Olympus, Japan) with a charge coupled device camera system at fixed exposure times for comparison. The statistical analyses of incorporation of GLUT 1 and eNOS in thoracic aortas were calculated using ImagePro Plus software (Bethesda, MD, USA).

2.11 Western blot analysis

The thoracic aorta specimens were homogenized in lysis buffer containing 0.1 mM phenylmethanesulfonyl as protease inhibitor,[27] loaded with 120 μg protein on 10% SDS polyacrylamide gel and then transferred into polyvinylidene difluoride membranes. Then, the proteins were transferred to polyvinylidene fluoride membranes and incubated with 5% bovine serum albumin to block non-specific binding. The membranes were incubated at 4 °C overnight and probed with eNOS-Ser^{1177}, Akt-Ser^{473} (dilution 1 : 1000), eNOS and Akt (dilution 1 : 200) as the target. After washing three times, the secondary antibody anti-rabbit IgG-conjugated horseradish peroxide (diluted 1 : 5000) was used to incubate the blots, the immunoreactivity was observed by chemiluminescence, and the relative expression was quantified.

2.12 Calculations and statistical analysis

Data are expressed as mean ± SEM, and n represents the number of animals. GraphPad Prism 5.0 software was used for statistical analysis. One-way analysis of variance (ANOVA) was used to compare the mean values of different groups, and SPSS 16.0 software was used for multiple comparisons. Two-tailed $p < 0.05$ was considered statistically significant ($\alpha = 0.05$).

2.13 Cell proliferation assay

The compounds (**1**, **3**, **4**, **7**, **8**, **9**, **11**, **12**, **19**, **21**, **23**, and **27**) were dissolved in dimethyl sulfoxide (DMSO) and, respectively, diluted to the required concentration (0.02, 0.2, 2, 20 mg mL^{-1}) using a culture solution. During the logarithmic phase of adherence of HUVECs, pancreatin was added. After dissociation, the culture solution was added (10% DMEM of fetal bovine serum), and this cell suspension was 105 units per mL. Suspension (100 μL) was added into each well of a 96-well culture plate and cultured for 24 h. The HUVECs were divided into 13 groups and each group was treated with L-NAME (100 μmol L^{-1}), L-NAME and compounds (**1**, **3**, **4**, **7**, **8**, **9**, **11**, **12**, **19**, **21**, **23**, **27**) for 24 h after the culture solution was removed, and with the control group only using culture solution. The supernatant was discarded and 10 μL of fresh MTT solution (5 mg mL^{-1}) was added into each well. After culturing for 4 h, the solution in each well was removed and mixed with 100 μL of DMSO. Optical density was measured at 570 nm using the enzyme-labeled instrument. Each concentration was repeated three times.

Cell survival rate (CSR) was measured by the MTT method, CSR% = (experiment group OD − blank group OD)/(control group OD − blank group OD) × 100%.

3. Results

3.1 Chemical analysis of BE

Compounds in the BE were identified by LC-MS analysis of mass-to-charge ratios and fragmentation (MS2) using data

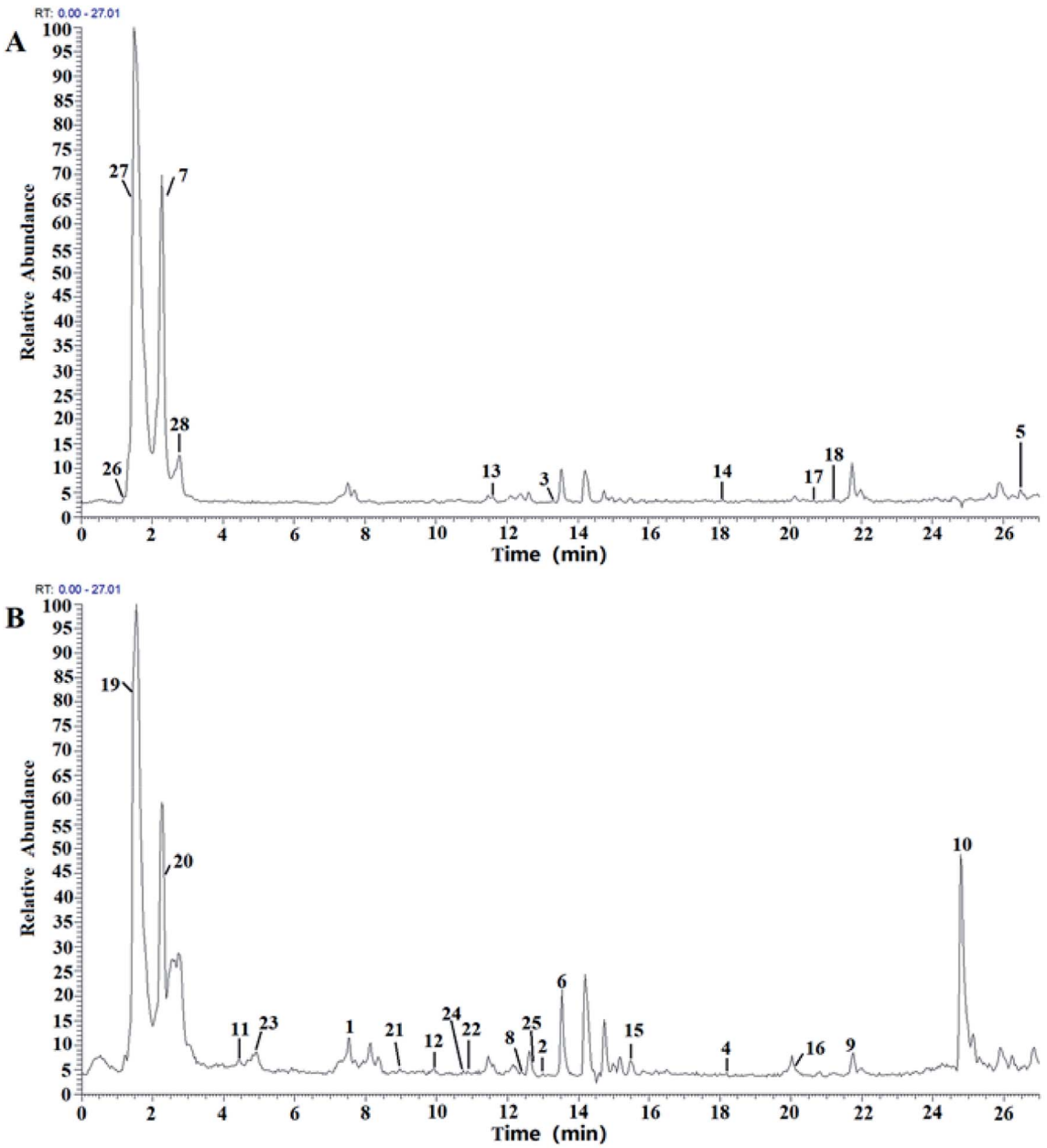

Fig. 2 LC-MS chromatograms of BE, in (A) positive-ion mode and (B) negative-ion mode.

Table 1 Chemical constituents identified in the ethanol ether extract of *Myrica rubra*

No.	t_R	Molecular formula	Selected ion	Experimental *m*/*z*	Theoretical *m*/*z*	Error (ppm)	MS/MS fragmentation (*m*/*z*)	Identification
1	7.77	$C_{20}H_{18}O_{11}$	$[M-H]^-$	433.0765	433.0765	0.000	301.2014, 273.0534, 244.8873	Quercetin-3-*O*-α-arabinopyranoside
2	13.09	$C_{21}H_{20}O_{12}$	$[M-H]^-$	463.0871	463.0878	−0.151	301.2014, 273.0534, 255.8373, 179.0340	Quercetin-3-*O*-galactoside
3	13.14	$C_{27}H_{30}O_{16}$	$[M+H]^+$	611.1606	611.1608	−0.327	303.3091, 163.0031	Rutin
4	18.25	$C_{15}H_{10}O_7$	$[M-H]^-$	301.0342	301.0349	2.063	285.0393, 257.0444, 229.0495, 165.0182	Quercetin
5	26.5	$C_{30}H_{40}O_{20}$	$[M+H]^+$	757.2185	757.2152	4.360	611.3409, 465.2311, 303.3091	Quercetin-3-*O*-2′,6′-dirhamnosylglucoside
6	13.49	$C_{21}H_{20}O_{12}$	$[M-H]^-$	463.0871	463.0878	−1.510	301.2014, 273.0534, 255.8373, 179.0340	Quercetin-7-*O*-β-D-glucoside
7	2.23	$C_{21}H_{20}O_{11}$	$[M+H]^+$	449.1078	449.1061	3.790	287.0117	Kaempferol-3-*O*-β-D-glucopyranoside
8	12.21	$C_{21}H_{18}O_{13}$	$[M-H]^-$	477.0663	477.0652	2.310	301.2014, 179.0340	Kaempferol-3-β-glucuronide
9	21.87	$C_{27}H_{30}O_{15}$	$[M-H]^-$	593.1500	593.1500	0.000	477.2924, 285.0925	Kaempferol-3-*O*-rutinoside
10	24.59	$C_{27}H_{30}O_{15}$	$[M-H]^-$	593.1500	593.1499	−0.170	285.0925	Kaempferol-3-*O*-D-glucopyranosyl-(1–2)-L-rhamnoside
11	4.24	$C_{15}H_{12}O_8$	$[M-H]^-$	319.0462	319.0456	4.354	150.9455, 180.9722	Dihydromyricetin
12	9.96	$C_{15}H_{10}O_8$	$[M-H]^-$	317.0301	317.0301	0.000	271.0694, 151.0343	Myricetin
13	11.49	$C_{21}H_{22}O_{12}$	$[M+H]^+$	467.1184	467.1170	3.000	303.3091, 229.0321	Morin-3-*O*-galactoside
14	18.15	$C_{15}H_{10}O_7$	$[M+H]^+$	303.0499	303.5000	−0.392	229.0321	Morin
15	15.43	$C_{16}H_{12}O_7$	$[M-H]^-$	315.0499	315.0504	−0.159	300.9910, 272.0534, 163.0390	Isorhamnetin
16	20.4	$C_{15}H_{12}O_5$	$[M-H]^-$	271.0600	271.0605	−0.174	187.8600, 165.0546	Naringenin
17	20.7	$C_{17}H_{14}O_7$	$[M+H]^+$	331.0812	331.0815	−0.910	253.0974	Cirsiliol
18	21.13	$C_{15}H_{10}O_6$	$[M+H]^+$	287.0550	287.0551	−0.350	139.0181	Luteolin
19	1.57	$C_4H_6O_5$	$[M-H]^-$	133.0134	133.0131	2.200	115.0025, 89.0232, 71.0127	DL-Malic acid
20	2.38	$C_6H_8O_7$	$[M-H]^-$	191.0192	191.0186	0.895	87.0076, 85.0283, 111.0076, 173.0081	Citric acid
21	8.9	$C_7H_6O_3$	$[M-H]^-$	137.0493	137.0233	2.600	93.0334, 65.0384	Salicylic acid
22	10.99	$C_7H_6O_4$	$[M-H]^-$	153.0186	153.0182	0.424	67.0178, 109.0283, 91.0178, 135.0077	2,4-Dihydroxybenzoic acid
23	4.07	$C_7H_6O_2$	$[M-H]^-$	169.0131	169.0135	−2.370	153.0182, 125.0961	Gallic acid
24	10.78	$C_9H_8O_4$	$[M-H]^-$	179.0338	179.0340	0.362	135.0441, 107.0489, 97.0281	Caffeic acid
25	13.16	$C_{10}H_{10}O_4$	$[M-H]^-$	193.0502	193.0495	1.216	149.0597, 134.0362, 90.9322, 61.9872	Ferulic acid
26	1.33	$C_6H_{14}N_4O_2$	$[M+H]^+$	175.1193	175.1189	2.043	158.0927, 130.0977, 116.071	DL-Arginine
27	1.52	$C_5H_7NO_3$	$[M+H]^+$	130.0501	130.0502	2.540	84.0450, 70.0658	L-Pyroglutamic acid
28	2.68	$C_9H_{11}NO_2$	$[M+H]^+$	166.0862	166.0862	0.200	120.0812, 103.0546	L-Phenylalanine

described in the literature and the GNPS database (Global Natural Products Social Molecular Networking). Negative-ion and positive-ion modes were used to identify the corresponding signals. A total of 28 compounds were identified, including 18 flavonoids[28–35] (compounds **1–18**), 8 organic acids (compounds **19–26**) and 3 amino acid (compounds **27–29**) (Fig. 2 and Table 1). The structures of all the identified compounds are shown in ESI Fig. S1.†

3.1.1 Quercetin derivatives. Quercetin generated the $[M + H]^+$ ion at *m/z* 303.0500 in the positive-ion mode, and the $[M - H]^-$ ion at *m/z* 301.0349 in the negative-ion mode. In the MS2 spectrum, it yielded *m/z* 285.0393 and 257.0444 by neutral loss of H_2O and H_2O + CO, and further yielded *m/z* 229.0495 and 165.0182 owing to retro Diels–Alder (RDA) rearrangement in the positive-ion mode.[36] Compounds **1–5** were identified as quercetin glycosides, which showed fragments common to those of quercetin and also gave specific fragmentation patterns corresponding to the loss of different substituents for each compound. For example, quercetin-3-*O*-2′,6′-dirhamnosylglucoside (**5**) showed the pseudomolecular ions of *m/z* 757.2152 $[M + H]^+$. The MS2 of *m/z* 757.2152 produced *m/z* 611.3409 $[M + H\text{-rha}]^+$, 465.2311 $[M + H\text{-2rha}]^+$, 303.3091 $[M + H\text{-2rha-glu}]^+$, 285.0760 and 257.0999 (Fig. S2†).

3.1.2 Kaempferol derivatives. Kaempferol is the dihydroxylation derivative of quercetin at the B ring of C3. It showed the pseudomolecular ion at *m/z* 287.0549, which was 16 Da less than that of quercetin. It produced a product ion at *m/z* 269.0453 $[M + H\text{–}H_2O]^+$ in the MS2 spectrum, and the ions at *m/z* 241.0496, 213.0549 and 165.0181 were related to the RDA fragmentation pathway.[36] A total of four kaempferol glycosides (compounds **7–10**) were identified. Compounds **9** and **10**, which were eluted at a retention time (t_R) of 21.87 and 24.59 min, respectively, showed the dominant protonated ion at *m/z* 593.1499 $[M - H]^-$. The MS2 spectrum of compound **9** presented fragment ions at *m/z* 447.2747 $[M - \text{H-rha}]^-$, 285.0925 $[M - \text{H-rha-glu}]^-$, 211.0119 and 163.0390, while compound **10** showed fragment ions at *m/z* 431.1392 $[M - \text{H-glu}]^-$ and 285.0925 $[M - \text{H-glu-rha}]^-$. The different fragmentation patterns above suggested that compounds **9** and **10** were kaempferol-3-*O*-rutinoside and kaempferol-3-*O*-D-glucopyranosyl-(1–2)-L-rhamnoside, respectively.

3.1.3 Myricetin derivatives. Myricetin showed pseudomolecular ions at *m/z* 317.0301 $[M - H]^-$. The MS2 spectrum showed product ions at *m/z* 271.0694 $[M - \text{H–}H_2O\text{–CO}]^-$ and 151.0343 $[M - \text{H–}C_8H_6O_4]^-$. Based on the observed common fragmentation pattern above, two myricetin derivatives (**11** and **12**) were also detected.

In addition, six flavonols with another aglycone, including isorhamnetin, two anthocyanidins (morin and morin-3-*O*-galactoside), cirsiliol, luteolin and naringenin were also identified, and the fragmentation pathways of these compounds were similar.

3.1.4 Organic acids and amino acid. The eight common organic acids or phenolics (compounds **19–25**) and three amino

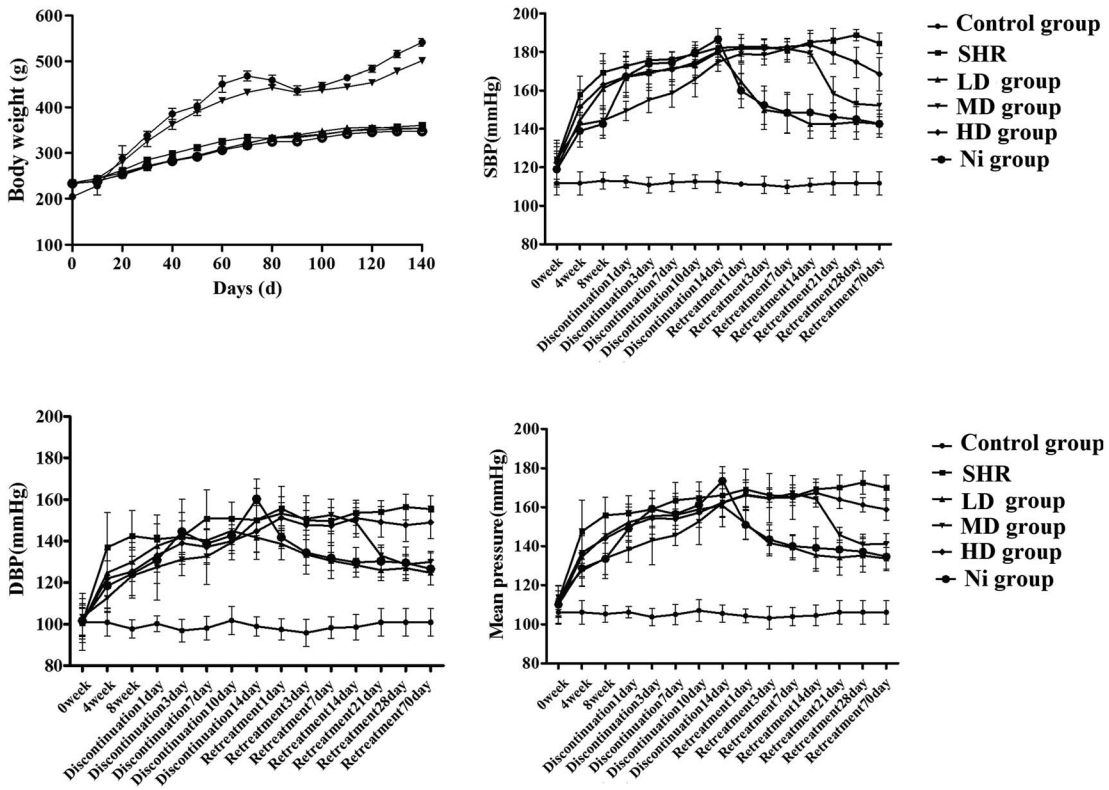

Fig. 3 Body weight and blood pressure from SHR rats treated with nifedipine (Ni) and bayberry extract (BE). (Top left) Body weight gain; (top right) systolic blood pressure, SBP; (bottom left) diastolic blood pressure, DBP; (bottom right) mean blood pressure, MBP.

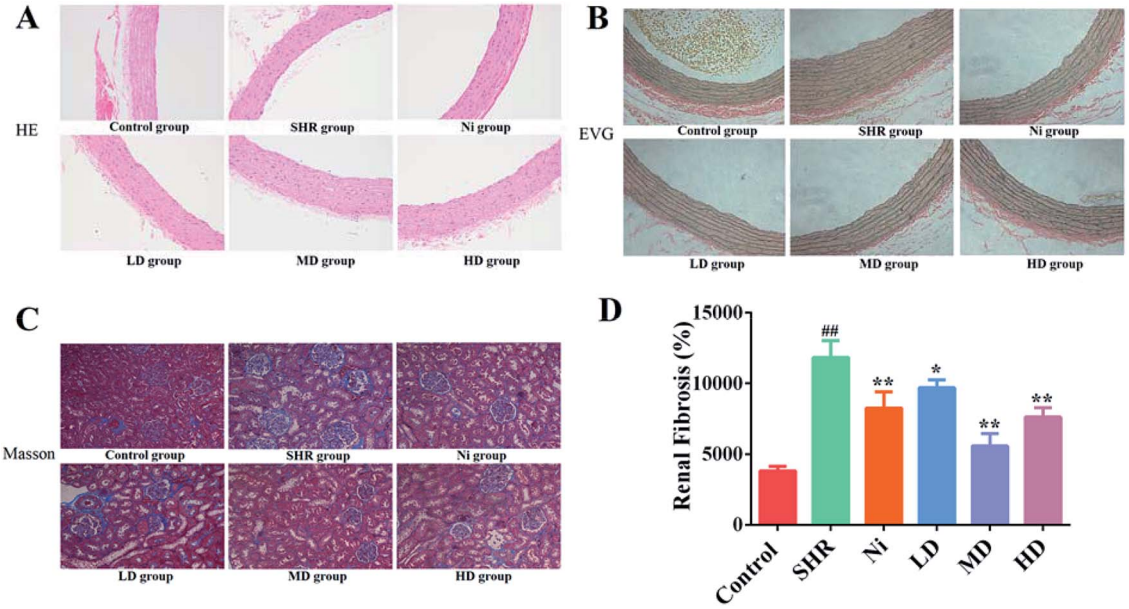

Fig. 4 Histopathological photomicrographs of thoracic aorta: (A) H&E staining and (B) EVG staining. (C) Masson's trichrome staining and (D) the calculation of renal fibrosis area. Ni, nifedipine group (10 mg kg^{-1}); LD, low dose group (1 g kg^{-1}); MD, middle dose group (2 g kg^{-1}); HD, high dose group (4 g kg^{-1}). Values are expressed as mean ± SEM ($n = 6$ rats). $^{\#\#}p < 0.01$ compared to normal group; $^{*}p < 0.05$; $^{**}p < 0.01$ compared to no treatment.

acids (**26–28**) were also identified in BE. Diagnostic mass fragments obtained in the negative mode at 133.0134, 191.0192, 137.0493, 153.0186, 169.0131, 179.0338 and 193.0502 characterized the aglycones as DL-malic acid, citric acid, salicylic acid (and 93.0334, 65.0384), 2,4-dihydroxybenzoic acid, gallic acid, caffeic acid, and ferulic acid, respectively. Furthermore, DL-arginine, L-pyroglutamic acid and L-phenylalanine were also identified in BE.

It is clear that flavonoids are the main components of BE.

3.2 Effect of BE on animal weight and blood pressure

As shown in Fig. 3 (top left), the bodyweight of each rat was recorded. In the control group, the body weight of the rats increased by 25% in 140 days. Administration of BE prevented SHR-induced loss of body weight, maintaining a near-normal weight, but Ni administration failed to do this.

Administration of nifedipine (10 mg kg^{-1}) resulted in a gradual decrease in blood pressure (BP) in the first week (DBP 12.8%, SBP 15.8%, MBP 13.3% *versus* the model group at the

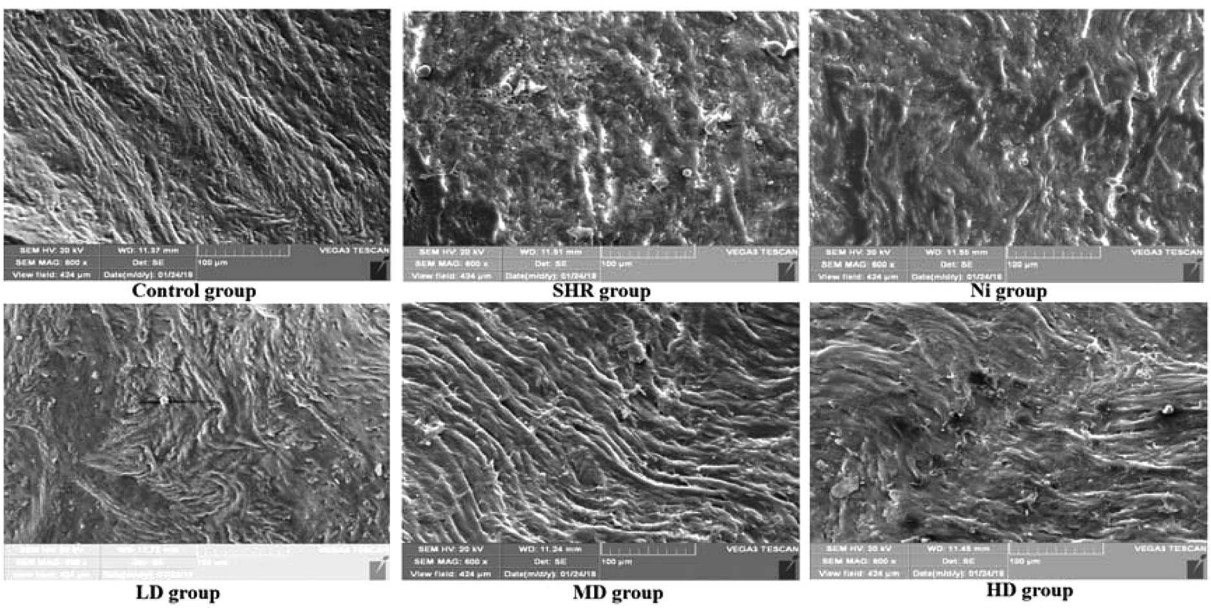

Fig. 5 SEM images of rat thoracic aorta: LD, low dose group (1 g kg^{-1}); MD, middle dose group (2 g kg^{-1}); HD, high dose group (4 g kg^{-1}).

end of eight weeks, $p < 0.01$). At the same time, after treatment with BE with a series of test concentrations, as shown in Fig. 3, those with increased blood pressure showed a significant reduction in blood pressure compared with the SHR group, until week 8 ($p < 0.01$). Then, treatment was discontinued for two weeks to determine the continuous curative effect. Surprisingly, a significant increase in blood pressure was observed in the Ni group compared with the control group, while the LD group (1 g kg^{-1}) and the MD group (2 g kg^{-1}) showed persistent modification of the pressure flex functions, accompanied by decreases in BP (Fig. 3). The blood pressure decreased rapidly after one day of retreatment with Ni, and its regulation was similar to that of the MD group ($p < 0.05$). However, blood pressure in the LD and HD groups was reduced until day 21 of retreatment, and blood pressure was higher than in the MD and Ni groups.

When the rats were given Ni at the same time, the negative effects were weakened in the early stage of blood pressure elevation (Fig. 3). Nevertheless, the increase in blood pressure during withdrawal illustrates that Ni has no significant effect. Compared with Ni, the effect of BE progresses slowly during treatment, but it can effectively reduce the SBP of SHR after stopping the drug (Fig. 3). A recent study[37] has shown rapid loss of vascular protection after discontinuation of Ni, with the result that systolic blood pressure returns to an abnormal value of SHR within 24 h. Our study indicates that BE was superior to endothelium-dependent vasodilation in Ni.

3.3 Pathological examination

The effects of BE on the cross-sectional area of the thoracic aorta in SHR rats was observed by H&E and EVG staining. The results of H&E staining showed that the endothelia of thoracic aorta were intact and smooth compared with SHR. The results for EVG staining indicated that the elastin wavy structure of the model group was disordered and the intima-media thickness was thickened compared with the control. After treatment with BE or Ni, the changes in SHR rats could be significantly attenuated, especially for the MD group (Fig. 4A).

The elastic tissue of the rat aortic wall can be visually stained using EVG staining.[38] Decreased relative elastin content in the aorta may lead to elevated blood pressure in spontaneously hypertensive rats.[39] It was reported that[40] vacuolar endothelium and incomplete circulating endothelial cells in the aorta of hypertensive rats destroyed the tissue structure. These results indicate that BE could restore the aortic wall of rats to maintain continued decrease in blood pressure (Fig. 4B).

There is much evidence that hypertension is a critical risk factor for chronic kidney disease and end-stage renal disease, which can lead to progression of renal fibrosis and renal failure.[41,42] Renal fibrosis is a key indicator for evaluating the effect of blood pressure. In order to find out whether there was a change in renal fibrosis after treatment administration, we performed a Masson's trichrome staining of kidney (Fig. 4C). The renal interstitial collagen deposition in the SHR group was significantly greater ($p < 0.01$) than in the control group. The degree of renal interstitial collagen deposition was reduced in

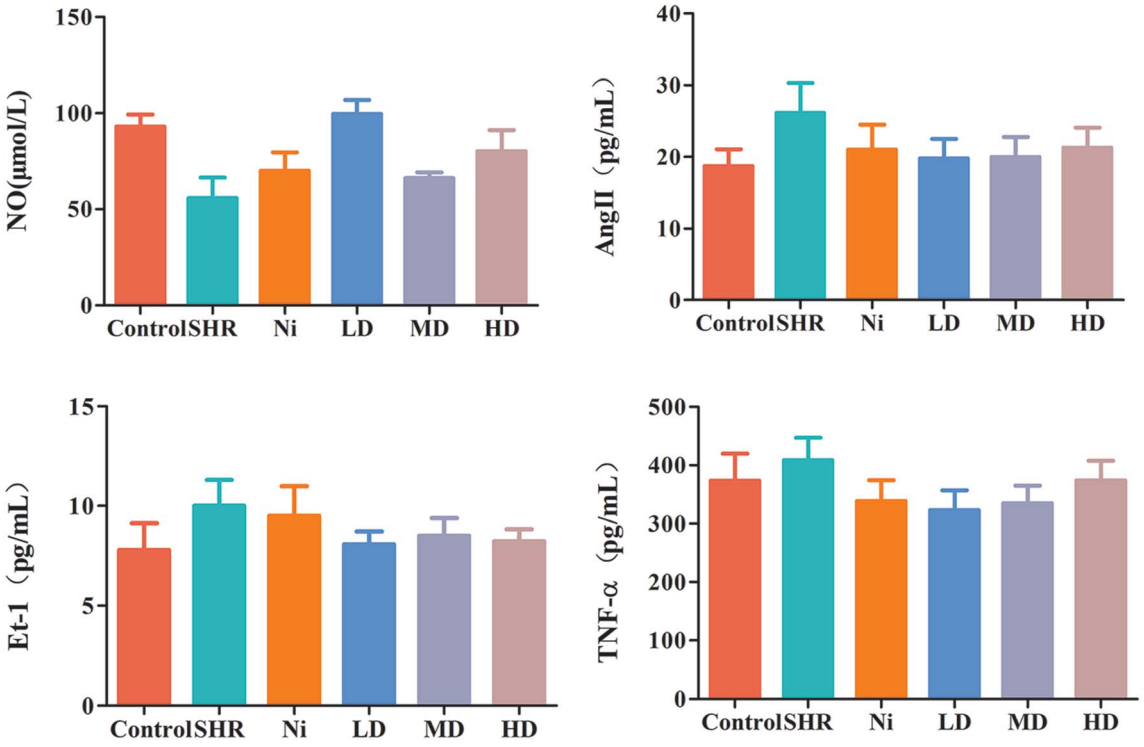

Fig. 6 Quantification of cytokines of NO, Ang II, Et-1 and TNF-α in serum as determined by ELISA. Results are representative of four individual experiments and expressed as mean ± SEM, with the significance accepted at $^{\#\#}p < 0.01$ *versus* control (no drug intervention). $^{*}p < 0.05$ and $^{**}p < 0.01$ *versus* only BE intervention group.

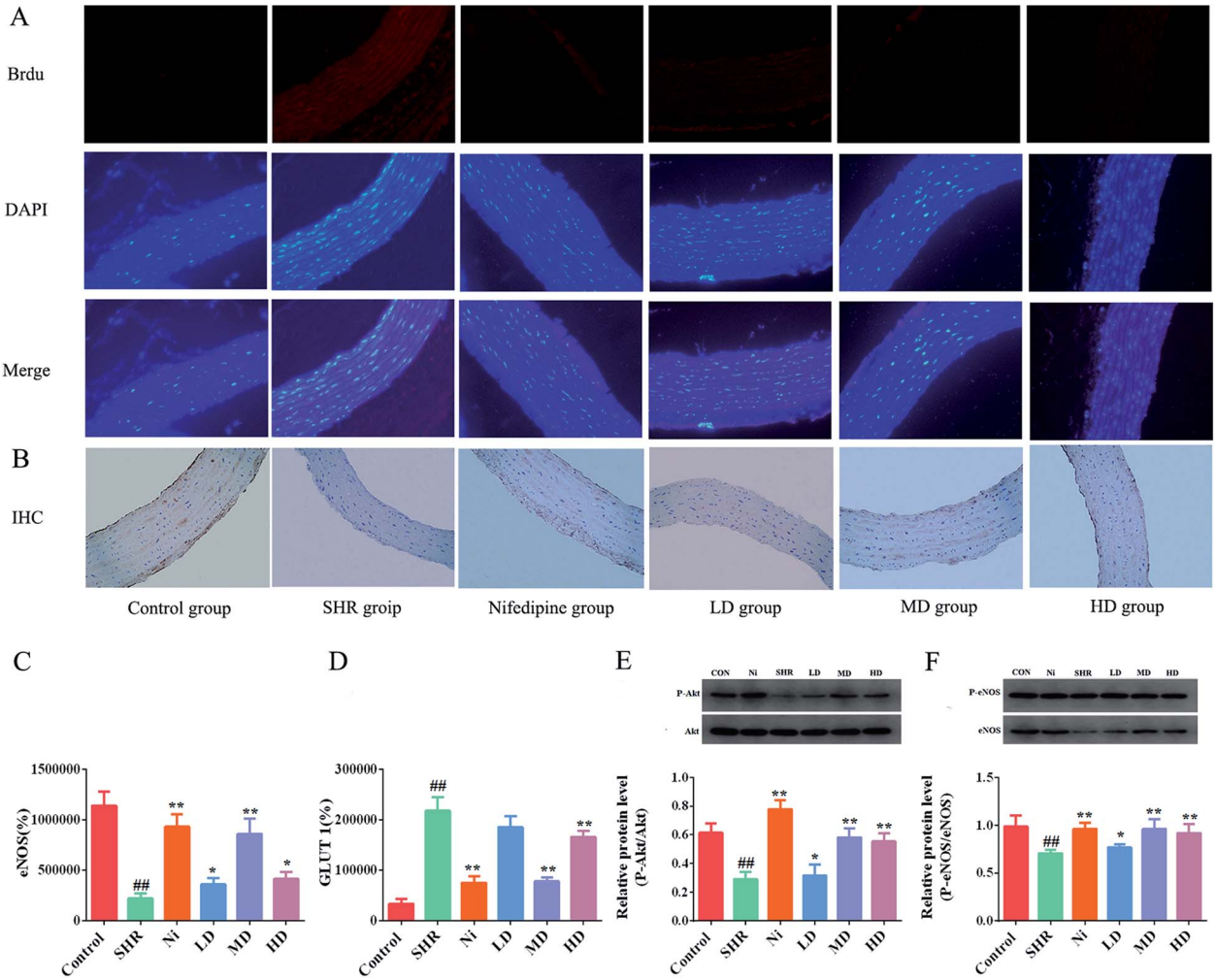

Fig. 7 Analysis determining the expression of phosphorylation of GLUT 1, eNOS, and Akt in vascular endothelium. (A) Immunofluorescence. (B) Immunohistochemical analysis. (C) Optical density of GLUT 1 immunofluorescence. (D) Area of eNOS immunohistochemistry. The levels of phosphorylation eNOS and total eNOS proteins were quantified by densitometry. (E) The levels of phosphorylation Akt and total Akt proteins were quantified by densitometry (F). Each value represents mean ± SEM and the significance accepted at $^{\#\#}$ indicates $p < 0.01$, compared with the respective normal control group. * and ** indicate $p < 0.05$ and $p < 0.01$, respectively, compared with the SHR group.

the drug-administered groups compared with the model group ($p < 0.05$).

3.4 Electron microscope scanning of thoracic aorta

Blood vessel endothelium could be clearly recognized by SEM. As shown in Fig. 5, well arranged and distributed blood vessels were observed in the control group. However, blood vessel endothelium disorders and damage could be found in the SHR group. This effect was attenuated after treatment with BE in the LD and MD dose groups. In particular, the regulatory effect in the MD group was almost the same as that of the control group.

3.5 Determination of biochemical markers

Several cytokines have been found to be closely related to hypertension, such as Ang II, ET-1 and TNF-α. Therefore, changes in these mediators in the model and treatment groups were tested by ELISA. The concentration of Ang II and ET-1 in the SHR group increased significantly ($p < 0.01$) (Fig. 6). The levels of Ang II and ET-1 were attenuated ($p < 0.05$) after treatment with BE at all concentrations tested. In addition, the level of TNF-α was decreased by treatment with BE (Fig. 6, bottom right). For these cytokines, the best regulatory effect was for the MD dose group and was similar to normal controls, and better than for Ni treatment.

Compared with the control group, the NO level in the SHR group was significantly decreased ($p < 0.01$), and it was significantly increased after treatment with LD or MD doses of BE. The MD group revealed a significant ($p < 0.01$) improvement, of about 78%, in the concentration of NO, and the curative effect was better than that of the Ni group (Fig. 6, top left).

3.6 Effects of BE on GLUT 1 and phosphorylation of Akt/eNOS pathway tissue

Most researchers consider that GLUT 1 is the main protein that promotes glucose transport across the plasma membranes of

Table 2 The docking scores of 28 active ingredients and GLUT1, eNOS, Akt, in BE

Target gene	PDB ID	Compound	Docking score	Compound	Docking score
GLUT 1	4JA4	Quercetin-3-*O*-α-arabinopyranoside	6.321	Isorhamnetin	3.549
eNOS	3EAH		5.431		4.219
AKT	3QKK		5.763		3.489
GLUT 1	4JA4	Quercetin-3-*O*-galactoside	5.212	Naringenin	5.342
eNOS	3EAH		4.211		5.216
AKT	3QKK		3.872		3.496
GLUT 1	4JA4	Rutin	7.651	Cirsilion	3.459
eNOS	3EAH		5.057		4.457
AKT	3QKK		5.941		4.398
GLUT 1	4JA4	Quercetin	5.972	Luteolin	3.459
eNOS	3EAH		6.258		4.457
AKT	3QKK		4.987		4.398
GLUT 1	4JA4	Quercetin-3-*O*-2′,6′-dirhamnosylglucoside	4.012	DL-Malic acid	4.485
eNOS	3EAH		3.521		5.296
AKT	3QKK		4.621		5.431
GLUT 1	4JA4	Hyperin	3.123	Citric acid	3.156
eNOS	3EAH		4.022		4.471
AKT	3QKK		4.316		4.137
GLUT 1	4JA4	Kaempferol-3-*O*-β-D-glucopyranoside	4.655	Salicylic acid	7.954
eNOS	3EAH		6.213		5.463
AKT	3QKK		5.232		6.954
GLUT 1	4JA4	Kaempferol-3-β-glucuronide	7.298	2,4-Dihydroxybenzoic acid	5.098
eNOS	3EAH		5.433		5.071
AKT	3QKK		5.008		5.413
GLUT 1	4JA4	Kaempferol-3-*O*-rutinoside	4.721	Gallic acid	4.651
eNOS	3EAH		5.071		4.072
AKT	3QKK		4.921		4.987
GLUT 1	4JA4	Kaempferol-3-*O*-D-glucopyranosyl-(1–2)-L-rhamnoside	4.442	Caffeic acid	3.265
eNOS	3EAH		3.143		4.594
AKT	3QKK		4.321		6.841
GLUT 1	4JA4	Dihydromyricetin	8.456	Ferulic acid	3.891
eNOS	3EAH		6.266		4.095
AKT	3QKK		6.461		4.397
GLUT 1	4JA4	Myricetin	7.951	DL-Arginine	5.713
eNOS	3EAH		6.335		5.342
AKT	3QKK		4.687		6.341
GLUT 1	4JA4	Morin-3-*O*-galactoside	4.123	L-Pyroglutamic acid	5.153
eNOS	3EAH		4.765		3.994
AKT	3QKK		3.065		3.074
GLUT 1	4JA4	Morin	4.321	L-Phenylalanine	4.485
eNOS	3EAH		4.544		5.296
AKT	3QKK		5.021		5.431

mammalian cells.[43] Overexpression of GLUT 1 leads to thickening of the vascular endothelium. Biological evidence suggested that eNOS is associated with hypertension, because it is a crucial regulator of cardiovascular homeostasis. eNOS regulates the basic vasodilation function of blood pressure by vascular endothelial catalysis of NO synthesis. In addition, by regulating blood vessel diameter, eNOS is a key factor affecting cardiovascular health, and has an anti-proliferative effect and provides an anti-apoptotic environment for cardiovascular disease.[44] Immunofluorescence analyses showed that the thoracic aortic level of the protein GLUT 1 was significantly elevated ($p < 0.01$) in SHR (Fig. 7A and D) compared with the control. Nevertheless, the expression of GLUT 1 in thoracic aorta of the BE group was significantly reduced. The GLUT 1 levels of the MD group showed a remarkable decrease of about 50%. On the other hand, eNOS did not increase in the SHR group, but sharply decreased (Fig. 7C and F) and the concentration of eNOS was elevated after administration with BE at all of the tested doses. It is worth noting that the levels of eNOS in the MD group were similar to those in the Ni group.

In vivo, Akt/protein kinase B plays a crucial role in regulating phosphorylation of eNOS-Ser^{1177}.[45] Previous studies have shown that the signaling pathway can be activated *in vitro*,[46] so we investigated whether the effects of BE on vasodilatation and vascular dysfunction were mediated through activation of eNOS-Ser^{1177} and Akt-Ser^{473} in the aorta. The Akt-Ser^{473} phosphorylation and total Akt expression in the aorta of the SHR group were reduced significantly compared with the normal controls ($p < 0.01$). As shown in Fig. 7E, after prophylactic administration with BE, the phosphorylation levels of Akt were

increased ($p < 0.05$). In addition, the medium dose group showed the best regulation effect with respect to normal controls, and its regulation effect was similar to that of Ni. The eNOS levels were increased while Akt-Ser^{473} phosphorylation was upregulated in the meantime. Compared with the control group, the level of eNOS in the SHR group was significantly lower ($p < 0.01$) and increased after treatment with BE at all tested doses. The MD group showed an obvious ($p < 0.05$) increase of about 35.8% in eNOS level, and the adjustment effect was similar to that of the Ni group (Fig. 7F).

3.7 Molecular docking analysis

Molecular docking analysis was also performed in order to explore the active ingredients in BE that had efficacy in hypertension. With GLUT 1, eNOS and Akt as target proteins we found their structures in the RCSB Protein Data Bank (http://www.rcsb.org/pdb/) and, along with the structures of the 28 compounds in BE, these were imported into system dock (http://systemsdock.unit.oist.jp/). On the basis of molecular docking, active ingredients of BE with tight binding to the protein target, using a docking score of >4.52,[47] were filtered out, and the scores are tabulated in Table 2. Twelve compounds identified in BE could be found to bind to GLUT 1, eNOS and Akt protein targets, indicating that these components were effective in treating hypertension by regulating GLUT 1, eNOS and Akt cytokines.

3.8 Compounds 3, 4, 11, 12, 23, and 27 increased cellular viability and stimulated NO production in HUVECs

In order to further explore the active substances of BE that have protective effects on blood vessels, we used the L-NAME-induced HUVECs hypertension model for MTT assay experiments. The results (Fig. S3†) show that compounds **3**, **4**, **11**, **12**, **23**, and **27** had obvious protective effects on L-NAME-induced HUVECs. However, there were three compounds (**7**, **19**, and **21**) that hardly protected HUVECs from damage, and compounds **1**, **7**, and **9** had a certain protective effect on the damage caused by L-NAME.

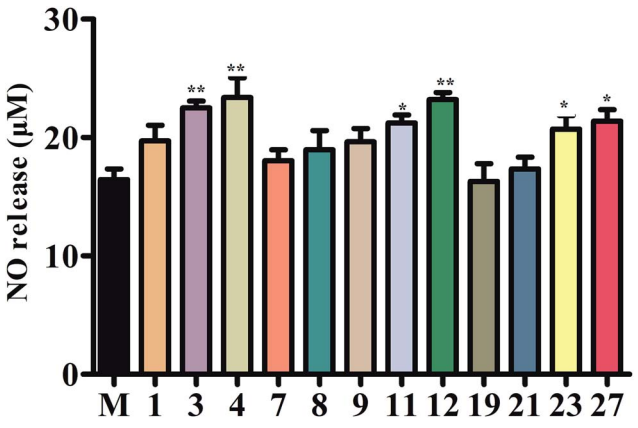

Fig. 8 The concentration of NO. Secreted NO was measured by the Griess assay in cell culture medium.

The concentration of NO is crucial in the progression of vascular dysfunction as well. Therefore, we measured the NO content in the supernatant fluid of the HUVEC culture medium. The levels of NO for compounds **3**, **4**, **11**, **12**, **23**, and **27** were significantly increased compared with the M (L-NAME) group. The NO release capacity was also increased by treatment with compounds **1**, **7**, or **9**, but showed no significant difference. In addition, compounds **7**, **9**, and **21** could not add to the capacity to release NO (Fig. 8).

In vitro study further revealed that compounds **3**, **4**, **11**, **12**, **23**, and **27** may play the most important role in antihypertensive effects. However, further *in vivo* studies are needed to validate these active compounds in BE.

4. Discussion

Angiotensin II is a peptide hormone of the renin–angiotensin–aldosterone system, which has pleiotropic effects on the vascular system and is a key mediator of hypertensive nephropathy. It plays a crucial role in the development of renal fibrosis and inflammation.[48] ET-1 is the most effective endogenous vasoconstrictor, and is strongly linked with the pathogenesis of hypertension.[18] In addition to increasing BP through vasoconstriction, ET-1 also contributes to the regulation of renal sodium and water, and causes vascular remodeling and endothelial dysfunction in the vascular system, which is common in hypertension. Therefore, blocking ET-1 may lower blood pressure and provide broader cardiovascular protection.[49] Several studies[50,51] have demonstrated that TNF-α levels in the serum of hypertensive patients were higher than those in healthy patients. Results suggest that BE could reduce the production of Ang II, ET-1 and TNF-α, which could lower inflammation and hypertension.

NO is a critical factor in maintaining various normal vascular functions in the cardiovascular system. It is regulated by means of vasodilatation and anti-atherosclerosis.[52] Decrease in NO bioavailability is considered to be a hallmark of endothelial dysfunction and plays a critical role in regulating blood pressure elevation.[53] It has been reported that direct inhibition of intrarenal NO can cause elevated blood pressure.[54] In this study, NO level was significantly increased after BE treatment, and the effect was close to that of the control group. These data indicate that the antihypertensive effect of BE was also associated with nutrition of endothelium function by eNOS/NO regulation.

GLUT 1 is a crucial enzyme regulating glucose metabolism.[55] In the past few decades, consumption of fructose has increased rapidly, and at the same time the incidence of hypertension has risen.[56] Glucose uptake is controlled by the surface level of glucose transporters and the activity of those transporters. Maher *et al.* revealed that GLUT 1 was overexpressed in brain microvascular endothelial cells of hypertensive patients.[57] In this study, GLUT 1 could be decreased by BE, which shows that BE had a better effect in maintaining normal vascular function.

Endothelial dysfunction is a characteristic of underlying vascular disease and can be simply defined as a decrease in the endothelium-dependent vasodilatation, suggesting that eNOS

levels are downregulated.[58] A previous study[59] has shown that Akt and eNOS phosphorylation play a key role in controlling vascular tone and controlling systolic blood pressure reduction. Our current results demonstrate that BE had a great protective effect on aortic endothelial function and promoted eNOS protein in the aorta. Our research provides strong evidence that BE is superior to Ni in endothelial-dependent vasodilation.

The Akt–eNOS pathway plays a crucial role in the endothelial function of the entire aorta, especially in the vascular endothelium. According to recent studies,[60,61] activation of Akt increases the effectiveness of NO by phosphorylation of eNOS at Ser^{1177}. The expression of p-Akt (Ser^{473}) and p-eNOS (Ser^{1177}) in vessel endothelia of SHR rats was significantly reduced after administration of BE. These data provide the vital statistical proof for maintaining hypertension, vascular structure damage, endothelial-associated vascular function, and inhabiting abnormal proliferation of smooth muscle cells. Meanwhile, the levels of NO in blood vessels of SHR rats were decreased, and increased after BE curing. Medical treatment enhanced the production of NO by increasing the expression of p-eNOS and p-Akt.[62] Thus, BE improved the endothelium-dependent vascular function mediated by Akt–eNOS phosphorylation, suggesting significant advantages in the continuous modification of baroreflex functions for BP reduction.

5. Conclusions

Our results confirmed the hypothesis that oral administration of ethanol extracts of bayberry could lower blood pressure in spontaneously hypertensive rats. Among 28 compounds identified in BE, 12 compounds (compounds **1**, **3**, **4**, **7–9**, **11**, **12**, **19**, **21**, **23**, and **27**) probably interacted with GLUT 1, eNOS and Akt for their antihypertensive effect. In a further *in vitro* study, compounds **3**, **4**, **11**, **12**, **23**, and **27** showed a significant protective effect on the L-NAME-induced HUVEC hypertension model. However, further *in vivo* studies are needed to validate the active compounds in BE. These results suggest that BE has an advantage in preventing hypertension compared with traditional therapies. The results presented here indicate that BE directly promotes NO release and eNOS activation in endothelial cells through the phosphorylation of Akt, and that BE plays a crucial role in controlling vascular remodeling in the pathogenesis of hypertension. Hypertension is one of the main symptoms of lifestyle-related diseases. Our results also indicate that *Myrica rubra*, as a functional food, has significant potential to prevent hypertension and its complications in daily life.

Ethics statement

All experiments in this study were carried out in accordance with the NIH Guide for the Care and Use of Laboratory Animals, and maximum efforts were made to minimize animal suffering and the number of animals necessary for the capture of reliable data.

Conflicts of interest

We confirm that this manuscript has not been published by another journal. All authors have approved the manuscript and agree with its submission to your journal. The authors declare that there is no conflict of interest regarding the publication of this paper.

Acknowledgements

We thank Scientific Instrument Center of Wuhan University for the LC-MS analysis.

References

1 T. Rajeshwari, B. Raja, J. Manivannan, *et al.*, Valproic acid prevents the deregulation of lipid metabolism and renal renin-angiotensin system in L-NAME induced nitric oxide deficient hypertensive rats, *Environ. Toxicol. Pharmacol.*, 2014, **37**, 936–945.

2 S. S. Lim, T. Vos, A. D. Flaxman, *et al.*, A comparative risk assessment of burden of disease and injury attributable to 67 risk factors and risk factor clusters in 21 regions, 1990-2010: a systematic analysis for the Global Burden of Disease Study 2010, *Lancet*, 2012, **380**, 2224–2260.

3 F. Dong, D. Wang, L. Pan, *et al.*, Disparities in Hypertension Prevalence, Awareness, Treatment and Control between Bouyei and Han: Results from a Bi-Ethnic Health Survey in Developing Regions from South China, *Int. J. Environ. Res. Public Health*, 2016, **13**, 233.

4 P. M. Kearney, M. Whelton, K. Reynolds, *et al.*, Global burden of hypertension: analysis of worldwide data, *Lancet*, 2005, **365**, 217–223.

5 A. Wirth, Z. Benyo, M. Lukasova, *et al.*, G12-G13-LARG-mediated signaling in vascular smooth muscle is required for salt-induced hypertension, *Nat. Med.*, 2008, **14**, 64–68.

6 A. C. Straub, A. W. Lohman, M. Billaud, *et al.*, Endothelial cell expression of haemoglobin alpha regulates nitric oxide signalling, *Nature*, 2012, **491**, 473–477.

7 J. F. Gielis, L. Quirynen, J. J. Briede, *et al.*, Pathogenetic role of endothelial nitric oxide synthase uncoupling during lung ischaemia-reperfusion injury, *Eur. J. Cardiothorac. Surg.*, 2017, **52**, 256–263.

8 U. Forstermann and W. C. Sessa, Nitric oxide synthases: regulation and function, *Eur. Heart J.*, 2012, **33**, 829–837, 837a.

9 Y. Zhou, W. P. Dirksen, G. J. Babu, *et al.*, Differential vasoconstrictions induced by angiotensin II: role of AT1 and AT2 receptors in isolated C57BL/6J mouse blood vessels, *Am. J. Physiol. Heart Circ. Physiol.*, 2003, **285**, H2797–H2803.

10 P. Fransen, C. E. Van Hove, A. J. Leloup, *et al.*, Effect of angiotensin II-induced arterial hypertension on the voltage-dependent contractions of mouse arteries, *Pflüg. Arch.*, 2016, **468**, 257–267.

11 A. Russell and S. Watts, Vascular reactivity of isolated thoracic aorta of the C57BL/6J mouse, *J. Pharmacol. Exp. Ther.*, 2000, **294**, 598–604.
12 R. E. Aluko, Antihypertensive peptides from food proteins, *Annu. Rev. Food Sci. Technol.*, 2015, **6**, 235–262.
13 Y. Solak, B. Afsar, N. D. Vaziri, *et al.*, Hypertension as an autoimmune and inflammatory disease, *Hypertens. Res.*, 2016, **39**, 567–573.
14 S. M. Krishnan, J. K. Dowling, Y. H. Ling, *et al.*, Inflammasome activity is essential for one kidney/deoxycorticosterone acetate/salt-induced hypertension in mice, *Br. J. Pharmacol.*, 2016, **173**, 752–765.
15 J. F. Navarro-González, C. Mora, M. Muros, *et al.*, Association of tumor necrosis factor-alpha with early target organ damage in newly diagnosed patients with essential hypertension, *J. Hypertens.*, 2008, **26**, 2168–2175.
16 H. L. Elliott, Gender differences with antihypertensive drug treatment, *J. Hypertens.*, 2002, **20**, 1491–1492.
17 H. Matsuda, T. Morikawa, J. Tao, *et al.*, Bioactive constituents of Chinese natural medicines. VII. Inhibitors of degranulation in RBL-2H3 cells and absolute stereostructures of three new diarylheptanoid glycosides from the bark of Myrica rubra, *Chem. Pharm. Bull.*, 2002, **50**, 208–215.
18 M. Yoshikawa, H. Shimada, N. Nishida, *et al.*, Antidiabetic principles of natural medicines. II. Aldose reductase and alpha-glucosidase inhibitors from Brazilian natural medicine, the leaves of Myrcia multiflora DC. (Myrtaceae): structures of myrciacitrins I and II and myrciaphenones A and B, *Chem. Pharm. Bull.*, 1998, **46**, 113–119.
19 H. Matsuda, T. Morikawa, J. Tao, *et al.*, Bioactive constituents of Chinese natural medicines. VII. Inhibitors of degranulation in RBL-2H3 cells and absolute stereostructures of three new diarylheptanoid glycosides from the bark of Myrica rubra, *Chem. Pharm. Bull.*, 2002, **50**, 208–215.
20 L. Xu, J. Gao, Y. Wang, *et al.*, Myrica rubra Extracts Protect the Liver from CCl(4)-Induced Damage, *J. Evidence-Based Complementary Altern. Med.*, 2011, **2011**, 518302.
21 N. Kumar, P. Bhandari, B. Singh, *et al.*, Antioxidant activity and ultra-performance LC-electrospray ionization-quadrupole time-of-flight mass spectrometry for phenolics-based fingerprinting of Rose species: Rosa damascena, Rosa bourboniana and Rosa brunonii, *Food Chem. Toxicol.*, 2009, **47**, 361–367.
22 J. Oszmianski, A. Wojdylo, J. Gorzelany, *et al.*, Identification and characterization of low molecular weight polyphenols in berry leaf extracts by HPLC-DAD and LC-ESI/MS, *J. Agric. Food Chem.*, 2011, **59**, 12830–12835.
23 H. X. Cui, J. H. Chen, J. W. Li, *et al.*, Protection of Anthocyanin from Myrica rubra against Cerebral Ischemia-Reperfusion Injury via Modulation of the TLR4/NF-kappaB and NLRP3 Pathways, *Molecules*, 2018, **23**, 1788–1799.
24 T. Inoue, Y. Arai and M. Nagai, Diarylheptanoids in the bark of Myrica rubra Sieb. et Zucc, *Yakugaku Zasshi*, 1984, **104**, 37–41.
25 T. Inoue, Constituents of Acer nikoense and Myrica rubra. On diarylheptanoids, *Yakugaku Zasshi*, 1993, **113**, 181–197.
26 A. J. Tipton, J. B. Musall, G. R. Crislip, *et al.*, Greater transforming growth factor-beta in adult female SHR is dependent on blood pressure, but does not account for sex differences in renal T-regulatory cells, *Am. J. Physiol. Renal. Physiol.*, 2017, **313**, F847–F853.
27 B. Piotrkowski, V. Calabro, M. Galleano, *et al.*, (-)-Epicatechin prevents alterations in the metabolism of superoxide anion and nitric oxide in the hearts of L-NAME-treated rats, *Food Funct.*, 2015, **6**, 155–161.
28 J. Wisniewski, M. G. Fleszar, J. Piechowicz, *et al.*, A novel mass spectrometry-based method for simultaneous determination of asymmetric and symmetric dimethylarginine, l-arginine and l-citrulline optimized for LC-MS-TOF and LC-MS/MS, *Biomed. Chromatogr.*, 2017, **31**, e3994.
29 Y. Shi, S. Tse, B. Rago, *et al.*, Quantification of fumarate and investigation of endogenous and exogenous fumarate stability in rat plasma by LC-MS/MS, *Bioanalysis*, 2016, **8**, 661–675.
30 M. Peitzsch, D. Pelzel, P. Lattke, *et al.*, Preservation of urine free catecholamines and their free O-methylated metabolites with citric acid as an alternative to hydrochloric acid for LC-MS/MS-based analyses, *Clin. Chem. Lab. Med.*, 2016, **54**, 37–43.
31 P. Purwaha, L. P. Silva, D. H. Hawke, *et al.*, An artifact in LC-MS/MS measurement of glutamine and glutamic acid: in-source cyclization to pyroglutamic acid, *Anal. Chem.*, 2014, **86**, 5633–5637.
32 L. Liu, X. Yin, X. Wang, *et al.*, Determination of dihydromyricetin in rat plasma by LC-MS/MS and its application to a pharmacokinetic study, *Pharm. Biol.*, 2017, **55**, 657–662.
33 J. Sun, F. Liang, Y. Bin, *et al.*, Screening non-colored phenolics in red wines using liquid chromatography/ultraviolet and mass spectrometry/mass spectrometry libraries, *Molecules*, 2007, **12**, 679–693.
34 J. Lee, B. L. S. Chan and A. E. Mitchell, Identification/quantification of free and bound phenolic acids in peel and pulp of apples (Malus domestica) using high resolution mass spectrometry (HRMS), *Food Chem.*, 2017, **215**, 301–310.
35 Z. Li, X. Guo, Z. Cao, *et al.*, New MS network analysis pattern for the rapid identification of constituents from traditional Chinese medicine prescription Lishukang capsules in vitro and in vivo based onUHPLC/Q-TOF-MS, *Talanta*, 2018, **189**, 606–621.
36 S. T. Yu, J. Li, L. Guo, *et al.*, Integrated liquid chromatography-mass spectrometry and nuclear magnetic resonance spectra for the comprehensive characterization of various components in the Shuxuening injection, *J. Chromatogr. A*, 2019, **1599**, 125–135.
37 V. Vaja, P. Ochodnicky, P. Krenek, *et al.*, Rapid large artery remodeling following the administration and withdrawal of calcium channel blockers in spontaneously hypertensive rats, *Eur. J. Pharmacol.*, 2009, **619**, 85–91.

38 K. Niwa, J. K. Perloff, S. M. Bhuta, *et al.*, Structural abnormalities of great arterial walls in congenital heart disease: light and electron microscopic analyses, *Circulation*, 2001, **103**, 393–400.
39 L. Xie, P. Lin, H. Xie and C. Xu, Effects of atorvastatin and losartan on monocrotaline-induced pulmonary artery remodeling in rats, *Clin. Exp. Hypertens.*, 2010, **32**, 547–554.
40 D. K. Sharma, A. Manral, V. Saini, *et al.*, Novel diallyldisulfide analogs ameliorate cardiovascular remodeling in rats with L-NAME-induced hypertension, *Eur. J. Pharmacol.*, 2012, **691**, 198–208.
41 Y. M. Barri, Hypertension and kidney disease: a deadly connection, *Curr. Hypertens. Rep.*, 2008, **10**, 39–45.
42 J. M. Krzesinski and E. P. Cohen, Hypertension and the kidney, *Acta Clin. Belg.*, 2007, **62**, 5–14.
43 A. L. Olson and J. E. Pessin, Structure, function, and regulation of the mammalian facilitative glucose transporter gene family, *Annu. Rev. Nutr.*, 1996, **16**, 235–256.
44 P. L. Huang, Z. Huang, H. Mashimo, *et al.*, Hypertension in mice lacking the gene for endothelial nitric oxide synthase, *Nature*, 1995, **377**, 239–242.
45 V. A. Morrow, F. Foufelle, J. M. Connell, *et al.*, Direct activation of AMP-activated protein kinase stimulates nitric-oxide synthesis in human aortic endothelial cells, *J. Biol. Chem.*, 2003, **278**, 31629–31639.
46 X. Li, J. Li, Z. Li, *et al.*, Fucoidan from Undaria pinnatifida prevents vascular dysfunction through PI3K/Akt/eNOS-dependent mechanisms in the L-NAME-induced hypertensive rat model, *Food Funct.*, 2016, **7**, 2398–2408.
47 K. Y. Hsin, S. Ghosh and H. Kitano, Combining machine learning systems and multiple docking simulation packages to improve docking prediction reliability for network pharmacology, *PLoS One*, 2013, **8**, e83922.
48 G. Liu, Y. Li, X. R. Huang, *et al.*, Smad7 inhibits AngII-mediated hypertensive nephropathy in a mouse model of hypertension, *Clin. Sci.*, 2014, **127**, 195–208.
49 T. Okura, M. Jotoku, J. Irita, *et al.*, Association between cystatin C and inflammation in patients with essential hypertension, *Clin. Exp. Nephrol.*, 2010, **14**, 584–588.
50 I. D. Bespalova, N. V. Riazantseva, V. V. Kaliuzhin, *et al.*, Effect of atorvastatin on pro-inflammatory status (in vivo and in vitro) in patients with essential hypertension and metabolic syndrome, *Kardiologiia*, 2014, **54**, 37–43.
51 R. C. Moorhouse, D. J. Webb, D. C. Kluth, *et al.*, Endothelin antagonism and its role in the treatment of hypertension, *Curr. Hypertens. Rep.*, 2013, **15**, 489–496.
52 J. Seo, J. Y. Lee, M. S. Sung, *et al.*, Arsenite Acutely Decreases Nitric Oxide Production via the ROS-Protein Phosphatase 1-Endothelial Nitric Oxide Synthase-Thr(497) Signaling Cascade, *Biomol. Ther.*, 2014, **22**, 510–518.
53 J. Davignon and P. Ganz, Role of endothelial dysfunction in atherosclerosis, *Circulation*, 2004, **109**, I27–I32.
54 D. S. Majid, S. A. Omoro, S. Y. Chin, *et al.*, Intrarenal nitric oxide activity and pressure natriuresis in anesthetized dogs, *Hypertension*, 1998, **32**, 266–272.
55 K. M. Pereira, F. N. Chaves, T. S. Viana, *et al.*, Oxygen metabolism in oral cancer: HIF and GLUTs (review), *Oncol. Lett.*, 2013, **6**, 311–316.
56 B. P. Marriott, N. Cole and E. Lee, National estimates of dietary fructose intake increased from 1977 to 2004 in the United States, *J. Nutr.*, 2009, **139**, 1228S–1235S.
57 F. Maher, S. J. Vannucci and I. A. Simpson, Glucose transporter proteins in brain, *FASEB J.*, 1994, **8**, 1003–1011.
58 J. A. Panza, P. R. Casino, D. M. Badar, *et al.*, Effect of increased availability of endothelium-derived nitric oxide precursor on endothelium-dependent vascular relaxation in normal subjects and in patients with essential hypertension, *Circulation*, 1993, **87**, 1475–1481.
59 Z. Shah, C. Pineda, T. Kampfrath, *et al.*, Acute DPP-4 inhibition modulates vascular tone through GLP-1 independent pathways, *Vasc. Pharmacol.*, 2011, **55**, 2–9.
60 S. Li, Q. Li, X. Lv, *et al.*, Aurantio-obtusin relaxes systemic arteries through endothelial PI3K/AKT/eNOS-dependent signaling pathway in rats, *J. Pharmacol. Sci.*, 2015, **128**, 108–115.
61 C. F. Garcia-Prieto, F. Hernandez-Nuno, D. D. Rio, *et al.*, High-fat diet induces endothelial dysfunction through a down-regulation of the endothelial AMPK-PI3K-Akt-eNOS pathway, *Mol. Nutr. Food Res.*, 2015, **59**, 520–532.
62 Z. Ying, X. Xie, M. Chen, K. Yi, *et al.*, Alpha-lipoic acid activates eNOS through activation of PI3-kinase/Akt signaling pathway, *Vasc. Pharmacol.*, 2015, **64**, 28–35.

